Free vibration analysis of in-plane circular curved beams with crack damage: a semi analytical solution

Xiaofei Li[a]* , Zhouyang Pan[a] , Haosen Zhai[a] , Dongyan Zhao[a]

[a] Colleage of Transportation Engineering, Dalian Maritime University, Dalian 116026, China. E-mails: lixiaofei@dlmu.edu.cn, panzhouyang@dlmu.edu.cn, zhs199608@163.com, zhaodongyan2021@dlmu.edu.cn

* Corresponding author

Abstract

In this paper, a semi-analytical method for solving circular curved beams is proposed to study the free vibration of in-plane circular curved beams in both undamaged and damaged configurations. The crack damage of the structure is represented by the cross-sectional reduction of the damaged element. Based on the discrete circular curved beam model, the coupling stiffness matrices of shear, compression and bending are derived. Combined with the lumped mass matrix and the dynamic characteristic equation of the multi-degree-of-freedom system, the frequencies and modes of the damaged and undamaged structures are calculated. The results are compared with the finite element method, and the good consistency between them is verified.
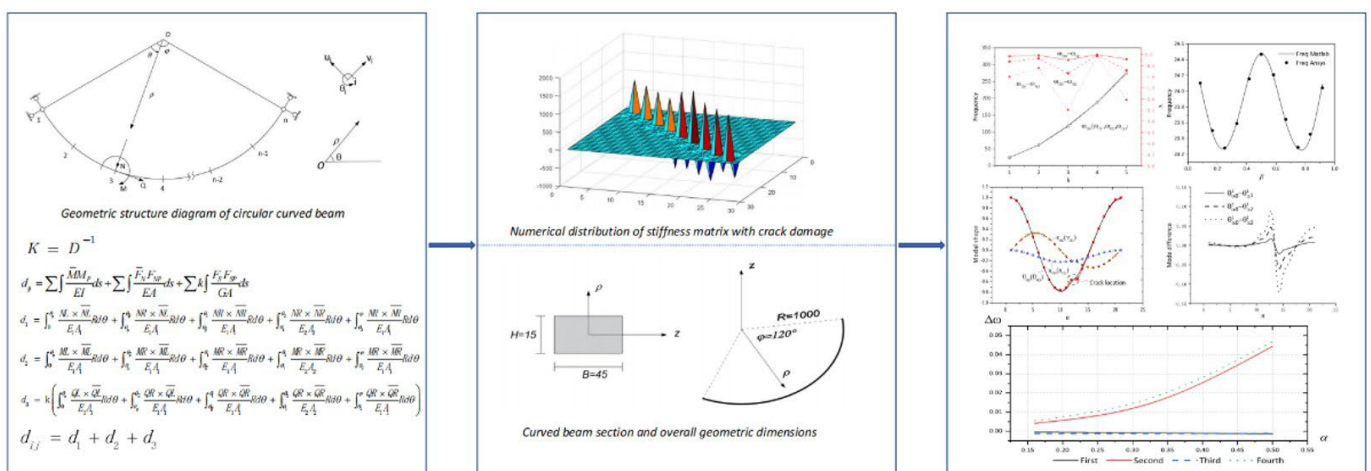
Keywords

Graphical Abstract

Geometric structure diagram of circular curved beam

Numerical distribution of stiffness matrix with crack damage

Curved beam section and overall geometric dimensions

1 INTRODUCTION

Curved beam structure is widely used in aerospace, mechanical, civil and other engineering (Zhao et al., 2006). In a complex working environment, the strength and stiffness of curved beam structure will decrease, and damage characteristics such as cracking and material weakening may occur, resulting in structural damage and safety accidents. So how to detect and identify the location and degree of structural damage has become an important research direction in curved beam damage identification. The occurrence of cracks in the structure will cause the change of local stiffness (Hu et al. (2007)), which will change the dynamic characteristics of the structure, thus affecting the natural frequency and vibration mode of the structure. Therefore, it is important to establish correct structure models both for the undamaged and the damaged structure in order to solve the frequency and vibration mode with certain accuracy.

The damage of structures is usually represented by the appearance of cracks. It can be found in some related articles. For example, Friswell and Penny (2002). There are roughly two methods for modeling cracks or crack-like defects in elastic beam structures. One is to introduce the concept of equivalent spring to simulate cracks. For example, (Rice and Levy (1972); Anifantis and Dimarogonas (1983); Chondros et al. (1998); Al-Said (2008)). The other is to reduce the relevant section size and simulate crack defects through notches in experiments. For example, (Dessi and Camerlengo (2015); Petroski (1981); Pau et al. (2011)). Based on the above methods, researchers have published many vibration studies of cracked beam structures with a large number of results. For example, (Wang et al. (2018); Anifantis and Dimarogonas (1983); Dimarogonas (1996)), which lay the foundation for the identification of cracks in beam structures. In addition, other crack modeling methods have also been developed, such as the uniform crack beam theory (Christides and Barr (1984); Shen and Pierre (1990)) and the nonlinear characteristics of breathing crack beams (Douka and Hadjileontiadis (2005); Chondros et al. (2001)).

Due to the influence of curvature, the plane curved beam structure leads to the coupling effect between internal forces, which is more complex than the straight beam. The dynamic research of cracked beam structure mainly focuses on the straight beam, while the curved beam structure has less research in this field. Krawzcuk and ostachowicz (1997) first analyzed the dynamic behavior of cracked curved beams, and studied the dynamic characteristics of circular arches with transverse cracks by using the finite element method. Viola et al. (2005) modeled the undamaged and damaged structures in the plane, proposed an exact analytical solution and an approximate numerical solution, and applied the two methods to solve for the intrinsic frequencies and vibration patterns of the circular arches to verify the consistency between them. Cerri et al (2008) also conducted an experimental study based on this and proposed an identification method based on frequency testing. Karaagac et al. (2011) established the finite element model of in-plane curved beam based on the energy method, and studied the influence of unilateral crack and its position on modal and dynamic stability. Caliò et al. (2016) Based on different damage modeling methods, the differences of different spatial arch models are evaluated. Eroglu and Tufekci (2017) used the concept of linear elastic fracture mechanics for crack modeling and exact solution of in-plane free vibrations of planar curved beams with crack is presented utilizing the transfer matrix method. Rezaiee-Pajand and Gharaei-Moghaddam (2020) proposed a force-based formula for cracked curved beam element, and formed a new cracked beam finite element, which verified the accuracy of the proposed element in calculating the frequency of cracked curved beam. Sun et al. (2021) carried out equal geometric free vibration analysis of curved Euler Bernoulli beams and obtained high-precision frequency solutions.

All the above-mentioned studies mainly use the finite element method (Krawzcuk and ostachowicz (1997); Krishnan et al. (1995); Raveendranath et al. (2000); Zhu and Meguid (2008); Rezaiee-Pajand and Gharaei-Moghaddam (2020) and analytical method (Viola et al. (2005); Qatu (1993); Khdeir and Reddy (1997); Tong et al. (1998); Tseng et al. (2000)) to solve the frequency and vibration mode of the curved beam witn damage. The latter requires the establishment of vibration differential equations for solution. Although the motion equation of curved beam can be solved accurately, due to different boundary conditions, different integral constants need to be solved, and it is only applicable to the solution of constant section, which has not been widely used in engineering. The finite element method is an approximate solution to solve the natural frequency and vibration mode of the damaged curved beam. The finite element method can effectively improve the calculation efficiency and obtain an approximate solution close to the exact solution. However, from its principle, its total stiffness matrix is usually integrated into a strip matrix distributed along the diagonal, with a large number of zero coupling terms, which is bound to bring some errors.

In this paper, from the perspective of structural discretization, the cracked circular curved beam model is established by the equivalent reduced section method, and the structural mechanics method and the principle of virtual work are used to solve for the structural flexibility matrix, and the overall stiffness matrix of the damaged circular curved beam is obtained after the matrix inversion. The structural characteristic equation is established and solved to obtain the natural frequency and vibration mode of the circular curved beam with crack. The frequency difference and vibration mode difference between undamaged and damaged structures were used to analyze the effect of single crack damage depth

and distribution on the disturbance of the frequency and vibration mode of the circular curved beam, to verify the effectiveness of the theoretical research applied to identify the damage of curved structures in this paper, and to provide a theoretical basis for the study of the dynamic characteristics of circular curved beams with damage and damage identification.

2 Analysis

2.1 Integrated stiffness matrix of in-plane circular curved beam with crack

According to structural mechanics, stiffness matrix and flexibility matrix are reciprocal matrices, and the specific relationship can be expressed as follows:

$$[K] = [D]^{-1} \tag{1}$$

Where [D] is the flexibility matrix of circular curved beam, [K] is the stiffness matrix.

The compliance matrix is an integrated matrix, which is obtained by integrating the internal force functions of statically indeterminate curved beam structure and statically determinate structure under unit loads in the directions of freedom in three planes.

Fig. 1 shows the stress model of a circular curved beam with simple support at both ends of the plane in polar coordinate system. The origin of the polar coordinate system is taken at the center of the circular curved beam structure. The polar diameter ρ is the radius of curvature of circular curved beam structure. Polar angle θ is the polar Angle coordinate of any section of the circular curved beam structure. The z-axis is perpendicular to the paper face and φ is the corresponding central Angle of the structure. The integral circular curved beam structure is separated into n nodes, and the allowable degrees of freedom of the nodes include radial translational displacement u, circumferential translational displacement v, and rotational angular displacement θ. The forms of external forces that can be applied to a node include radial force, circumferential force, and couple force. The internal forces produced by the full-beam section include radial shear Q, circumferential axial force N, and bending moment M.
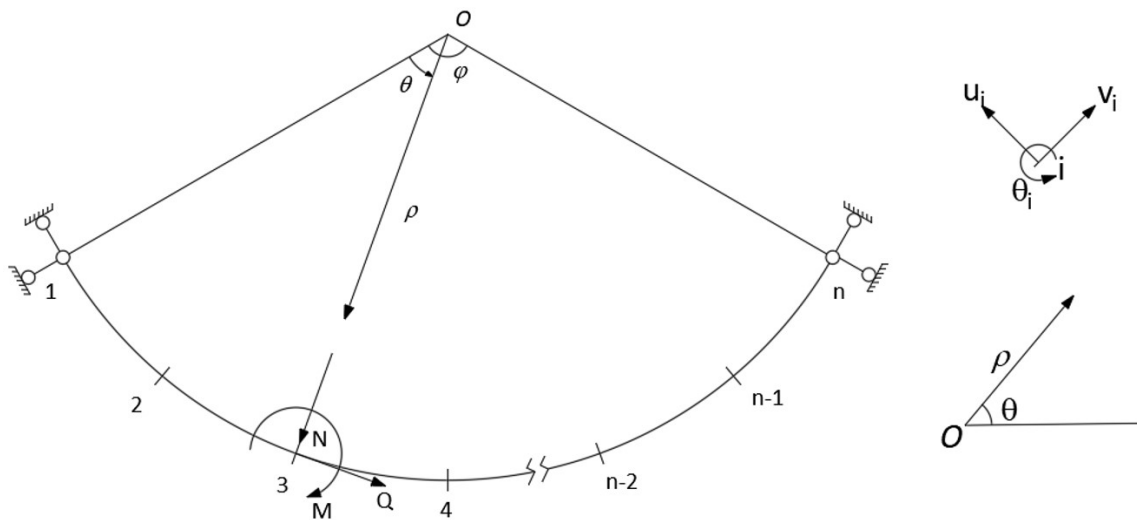
Figure 1 Geometric structure diagram of circular curved beam

In this paper, crack damage in curved beams is studied. In order to show the weakening effect of damage on the section properties of curved beams, the curved beams are divided into three sections, that is, $[0, \theta_1]$; $[\theta_1, \theta_2]$ and $[\theta_2, \theta_3]$ are denoted as cross-section area A_1, elastic modulus E_1, shear modulus G_1 in the first and third sections, and A_2, E_2, G_2 in the second section. Since the solution of the internal force function depends on the calculation of the reaction force of the support and is affected by the position of the external load, it is discussed in this case.

It should be noted that the unit loads in the three degrees of freedom directions in the plane need to act on the three sections in turn. This is because the solution of the bearing reaction force is related to the section properties. The solution process of the whole flexibility coefficient is a cyclic process. The following is a brief introduction to the solution process.
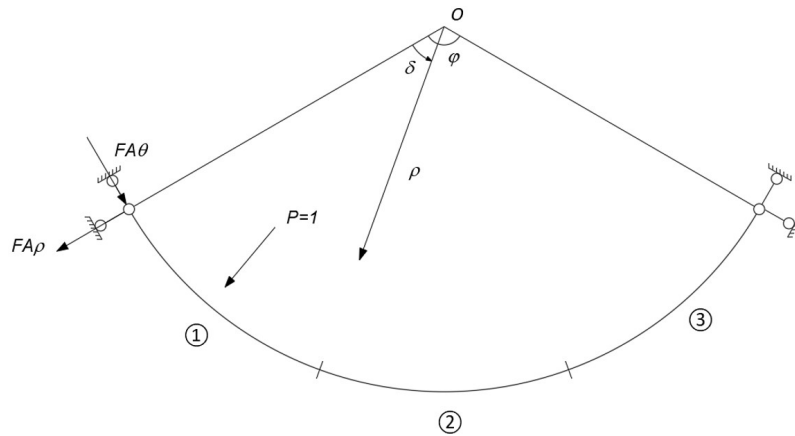
Figure 2 Force analysis diagram of statically indeterminate curved beam structure under unit radial force

When radial unit load P=1 acts on point $\left[0,\theta_1\right]$, the circumferential redundant force $F_{A\theta}$ and radial support reaction force $F_{A\rho}$ are solved by force method, and the internal force function of statically indeterminable structure is established based on structural geometric relations. As shown in Figure 2.

$$\begin{cases} NL(\delta) = -F_{A\rho}\sin\delta + F_{A\theta}\cos\delta \\ ML(\delta) = R[-F_{A\rho}\sin\delta + F_{A\theta}(1-\cos\delta)] \quad \left(0 \leq \delta \leq \theta_p\right) \\ QL(\delta) = -F_{A\rho}\cos\delta - F_{A\theta}\sin\delta \end{cases}$$

$$\begin{cases} NR(\delta) = NL(\delta) - \sin(\delta - \theta_p) \\ MR(\delta) = ML(\delta) - R\sin(\delta - \theta_p) \quad \left(\theta_p \leq \delta \leq \varphi\right) \\ QR(\delta) = QL(\delta) - \cos(\delta - \theta_p) \end{cases}$$

(2)
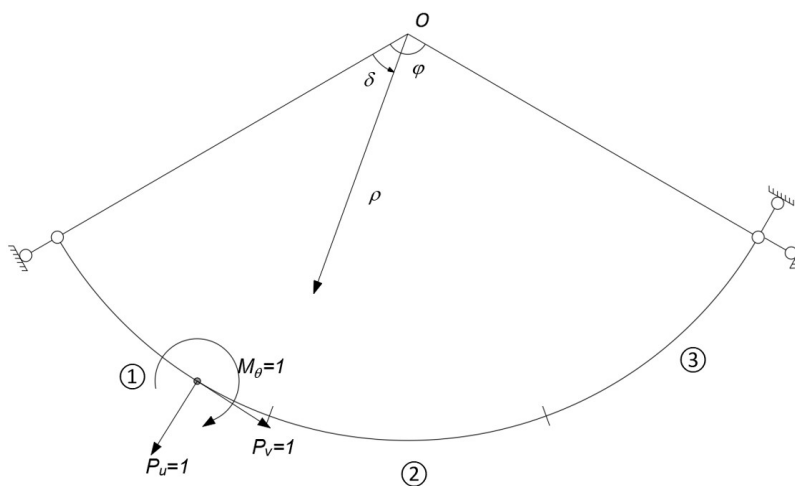
Figure 3 Force diagram of statically fixed curved beam structure

There are three internal force functions of statically determinate structure under in-plane unit load. As shown in Figure 3.

Under unit radial force:

$$
\begin{cases}
\overline{NL}(\delta) = \dfrac{\sin\left(\varphi - \theta_{\bar{p}}\right)}{\sin\varphi}\sin\delta \\[4mm]
\overline{ML}(\delta) = \dfrac{\sin\left(\varphi - \theta_{\bar{p}}\right)}{\sin\varphi}R\sin\delta \qquad \left(\delta \le \theta_{\bar{p}}\right)\\[4mm]
\overline{QL}(\delta) = \dfrac{\sin\left(\varphi - \theta_{\bar{p}}\right)}{\sin\varphi}\cos\delta
\end{cases}
\qquad
\begin{cases}
\overline{NR}(\delta) = \overline{NL}(\delta) - \sin\left(\delta - \theta_{\bar{p}}\right)\\[3mm]
\overline{MR}(\delta) = \overline{ML}(\delta) - R\sin\left(\delta - \theta_{\bar{p}}\right) \qquad \left(\delta \ge \theta_{\bar{p}}\right)\\[3mm]
\overline{QR}(\delta) = \overline{QL}(\delta) - \cos\left(\delta - \theta_{\bar{p}}\right)
\end{cases}
\tag{3}
$$

Under unit tangential force:

$$
\begin{cases}
\overline{NL}(\delta) = \dfrac{1 - \cos\left(\varphi - \theta_{\bar{p}}\right)}{\sin\varphi}\sin\delta \\[4mm]
\overline{ML}(\delta) = \dfrac{1 - \cos\left(\varphi - \theta_{\bar{p}}\right)}{\sin\varphi}R\sin\delta \qquad \left(\delta \le \theta_{\bar{p}}\right)\\[4mm]
\overline{QL}(\delta) = \dfrac{1 - \cos\left(\varphi - \theta_{\bar{p}}\right)}{\sin\varphi}\cos\delta
\end{cases}
\qquad
\begin{cases}
\overline{NR}(\delta) = \overline{NL}(\delta) + \cos\left(\delta - \theta_{\bar{p}}\right)\\[3mm]
\overline{MR}(\delta) = \overline{ML}(\delta) - \left[R - R\cos\left(\delta - \theta_{\bar{p}}\right)\right] \qquad \left(\delta \ge \theta_{\bar{p}}\right)\\[3mm]
\overline{QR}(\delta) = \overline{QL}(\delta) - \sin\left(\delta - \theta_{\bar{p}}\right)
\end{cases}
\tag{4}
$$

Under the action of unit couple:

$$
\begin{cases}
\overline{NL}(\delta) = \dfrac{\sin\delta}{R\sin\varphi} \\[4mm]
\overline{ML}(\delta) = \dfrac{\sin\delta}{\sin\varphi} \qquad \left(\delta \le \theta_{\bar{p}}\right)\\[4mm]
\overline{QL}(\delta) = \dfrac{\cos\delta}{R\sin\varphi}
\end{cases}
\qquad
\begin{cases}
\overline{NR}(\delta) = \overline{NL}(\delta)\\[3mm]
\overline{MR}(\delta) = \overline{ML}(\delta) - 1 \qquad \left(\delta \ge \theta_{\bar{p}}\right)\\[3mm]
\overline{QR}(\delta) = \overline{QL}(\delta)
\end{cases}
\tag{5}
$$

Due to different integral intervals, the piecewise integral summation operation of the above internal force functions is needed to obtain the compliance element d_{ij} of row i and column j when using the displacement integral formula.

$$
d_{ij} = \sum\int\frac{\overline{M}M_P}{EI}ds + \sum\int\frac{\overline{F}_N F_{NP}}{EA}ds + \sum k\int\frac{F_S F_{SP}}{GA}ds
\tag{6}
$$

Through the above calculation, the radial uncoupled compliance matrix, radial - circumferential coupled compliance matrix, and radial - rotational coupled compliance matrix can be obtained. Similarly, formula (2)-(6) is used to calculate the displacement summation in cases $\theta_p \in \left[\theta_1, \theta_2\right]$ and $\theta_p \in \left[\theta_2, \varphi\right]$ respectively. Numbered according to the degree of freedom of nodes: 1-radial translational displacement, 2-circumferential translational displacement and 3-rotational angular displacement. The obtained structure is integrated into the flexibility matrix of order according to the coordinate numbering. According to the coordinate numbering, the obtained results is integrated into the 3n×3n order flexibility matrix. The interval $\left[\theta_1, \theta_2\right]$ is represented as the damaged element, and the two ends of the element are polar Angle coordinate. The section parameters of the element are changed to characterize the section crack damage of the circular curved beam structure.

$$
\left[D_{\rho\rho}\right] = \begin{bmatrix} d_{22} & d_{25} & d_{28} \\ d_{52} & d_{55} & d_{58} \\ d_{82} & d_{85} & d_{88} \end{bmatrix}
\tag{7}
$$

Equation (7) lists the solution process of the radial uncoupled flexibility matrix $\left[D_{\rho\rho}\right]$ of the 5-node circular curved beam structure, in which the calculation of the flexibility elements should consider the integration interval and integration order. If θ_{p} and $\theta_{\overline{\mathrm{p}}}$ are both in the interval $[0,\theta_1]$, and $\theta_{\mathrm{p}} \le \theta_{\overline{\mathrm{p}}}$, it can be known from equations (3) and (6).

$$d_1 = \int_0^{\theta_\mathrm{p}} \frac{NL \times \overline{NL}}{E_1 A_1} R d\theta + \int_{\theta_\mathrm{p}}^{\theta_{\overline{\mathrm{p}}}} \frac{NR \times \overline{NL}}{E_1 A_1} R d\theta + \int_{\theta_{\overline{\mathrm{p}}}}^{\theta_1} \frac{NR \times \overline{NR}}{E_1 A_1} R d\theta + \int_{\theta_1}^{\theta_2} \frac{NR \times \overline{NR}}{E_2 A_2} R d\theta + \int_{\theta_2}^{\varphi} \frac{NR \times \overline{NR}}{E_1 A_1} R d\theta \tag{8}$$

$$d_2 = \int_0^{\theta_\mathrm{p}} \frac{ML \times \overline{ML}}{E_1 A_1} R d\theta + \int_{\theta_\mathrm{p}}^{\theta_{\overline{\mathrm{p}}}} \frac{MR \times \overline{ML}}{E_1 A_1} R d\theta + \int_{\theta_{\overline{\mathrm{p}}}}^{\theta_1} \frac{MR \times \overline{MR}}{E_1 A_1} R d\theta + \int_{\theta_1}^{\theta_2} \frac{MR \times \overline{MR}}{E_2 A_2} R d\theta + \int_{\theta_2}^{\varphi} \frac{MR \times \overline{MR}}{E_1 A_1} R d\theta \tag{9}$$

$$d_3 = k \left(\int_0^{\theta_\mathrm{p}} \frac{QL \times \overline{QL}}{E_1 A_1} R d\theta + \int_{\theta_\mathrm{p}}^{\theta_{\overline{\mathrm{p}}}} \frac{QR \times \overline{QL}}{E_1 A_1} R d\theta + \int_{\theta_{\overline{\mathrm{p}}}}^{\theta_1} \frac{QR \times \overline{QR}}{E_1 A_1} R d\theta + \int_{\theta_1}^{\theta_2} \frac{QR \times \overline{QR}}{E_2 A_2} R d\theta + \int_{\theta_2}^{\varphi} \frac{QR \times \overline{QR}}{E_1 A_1} R d\theta \right) \tag{10}$$

The flexibility element is solved as follows:

$$d_{ij} = d_1 + d_2 + d_3 \tag{11}$$

According to Equation (1), the exact stiffness matrix with damage can be obtained by inverse matrix operation [D]. The numerical distribution of the stiffness matrix [K] is shown in Fig. 2:
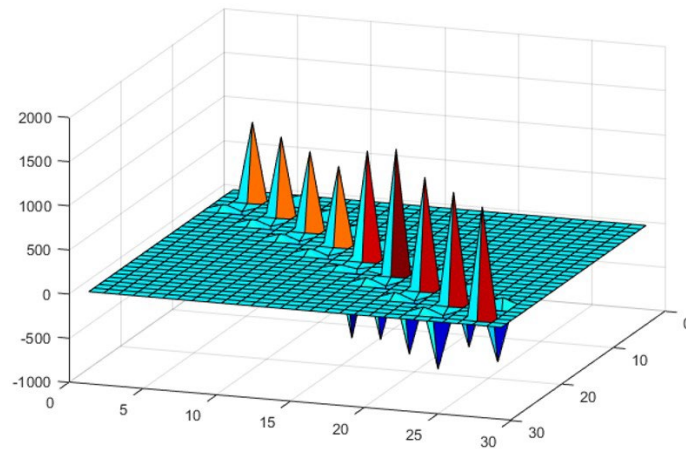
Figure 4 Numerical distribution of stiffness matrix with crack damage

As can be seen from the figure 4, the highest peak of the main diagonal is the coefficient term related to the rotational stiffness, which is much higher than other translational stiffness values. Due to the uneven distribution of the element grid at the damage location and the change of section properties at the damage, the stiffness value distribution presents the phenomenon of high and low. The peak value mutation is the damage position of the circular curved beam structure, which is due to the reduction of the unit section, resulting in the change of stiffness.

2.2 Integrated mass matrix with crack damage

The mass matrix of the circular curved beam structure is integrated by lumped mass method. The mass matrix integrated by the lumped mass method is usually a diagonal matrix distributed along the main diagonal without considering the coupling relationship between rotational mass and translational mass. The simplified lumped mass model of statically in indestructed in-plane circular curved beam structure is shown in Fig. 5.
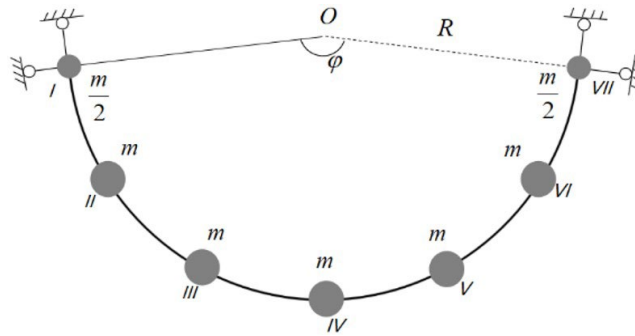
Figure 5 Mass distribution of circular curved beams

The circular curved beam structure is divided into sections, and the nodes are taken as the connecting points. It is assumed that each arc mass accumulates into point mass at each node, and the mass allocated to each node is determined by statics. Its lumped mass matrix is:

$$[M] = \begin{bmatrix} m_1 & 0 & 0 & \dots & \dots & \dots & 0 & 0 & 0 \\ 0 & m_2 & 0 & \dots & \dots & \dots & 0 & 0 & 0 \\ 0 & 0 & j_3 & \dots & \dots & \dots & 0 & 0 & 0 \\ & & & \dots & & & & & \\ & & & & \dots & & & & \\ & & & & & \dots & & & \\ 0 & 0 & 0 & \dots & \dots & \dots & m_{3n-2} & 0 & 0 \\ 0 & 0 & 0 & \dots & \dots & \dots & 0 & m_{3n-1} & 0 \\ 0 & 0 & 0 & \dots & \dots & \dots & 0 & 0 & j_{3n} \end{bmatrix} \quad (12)$$

After eliminating the mass coefficient corresponding to the constraint, the number of diagonal items in the matrix is equal to the freedom degree of the circular curved beam. m_i represents translational mass, and j_i represents the moment of inertia of the rigid body.

2.3 Natural vibration analysis of In-plane circular curved beam

In the undamped modal analysis of circular curved beam structures, the required structural characteristic matrices are stiffness matrix [K] and mass matrix [M]. The modal calculation of circular curved beam belongs to the eigenvalue problem in mathematics. The governing equation of its structural characteristics is:

$$K\phi = \lambda M\phi \quad (13)$$

In the formula, λ is the eigenvalue corresponding to the natural vibration frequency of the structure, ϕ and is the structural modal vector corresponding to the eigenvector.

3 The example analysis

In order to verify the calculation results, a specific example is introduced, as shown in Figure 6. The calculation example uses a rectangular section constant curvature curved beam simply supported at both ends, with section height h=15mm, section width b=45mm, Sectional area A=675mm^2. The physical parameters of the circular curved beam without damage state are shown in Table 1.
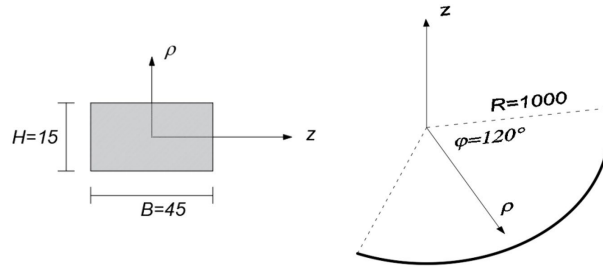
Figure 6 Curved beam section and overall geometric dimensions

Table 1 Physical geometric parameters of circular curved beam

Characteristic properties	Values
Section height, h	45mm
Breadth of section, b	15mm
Central Angle of a curved beam, φ	120°
Radius of the axis of the arch, R	1000mm
Young's modulus, E	2.06×10^5Mpa
Shear modulus, G	8.0×10^4Mpa
Relevant moment of inertia of the cross-section, I	1.14×10^5mm⁴
Shearing factor, k	1.2

3.1 Natural vibration analysis of In-plane circular curved beam

The circular curved beam model is divided into 20 segments with a total of 21 nodes, as shown in fig 7. It is assumed that the range of the damage element is $\left[\theta_1, \theta_2\right]$, and the crack section height is reduced to simulate the stiffness weakening of the beam segment. The damage degree at the structural crack is defined as follows:

$$\alpha = \frac{h_d}{h} \tag{14}$$

$$\beta = \frac{\theta_2 - \theta_1}{2\varphi} \tag{15}$$

Where α is the damage degree coefficient, and h_d is the section height of crack damaged beam element. β Characterize the section position of crack damage.
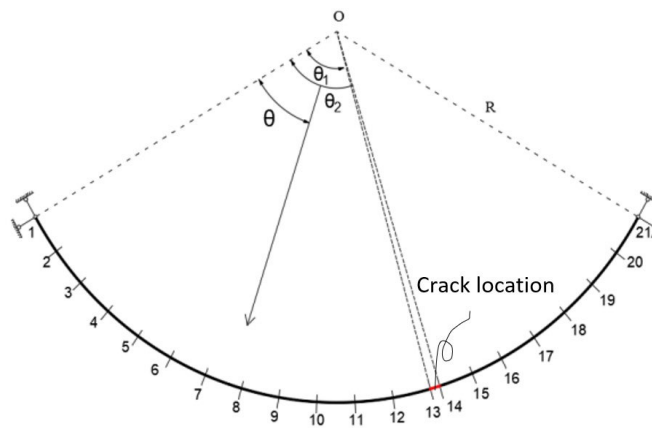
Figure 7 Damaged circular curved beam model with crack

The method above is applied to solve the frequency value of the circular curved beam at $\alpha_1 = 0.16$、 $\alpha_2 = 0.33$、 $\alpha_3 = 0.5$ and no damage state. In order to verify the effectiveness of the proposed method in analyzing the free vibration of circular curved beams with different damage degrees, a finite element model was established for the above problems, and its numerical solution was obtained. The frequency values obtained by the two methods are listed in Table 2. Through the results of the two methods, it can be seen that the larger the damage coefficient is, the smaller the natural vibration frequency is. The solution in this paper has the same trend as that of the finite element method. The error values of the two methods indicate that the frequency values of each order obtained by using the precise algorithm in this paper maintain excellent and stable solutions under different damage coefficient. The correctness of the proposed method for solving the dynamic characteristics of damaged circular curved beams is verified.

Table 2 Natural frequency of circular curved beam with crack damage

Mode	Frequency ($\propto = 0$)		error/ (%)	Frequency ($\propto = 0.16$)		error/ (%)	Frequency ($\propto = 0.33$)		error/ (%)	Frequency ($\propto = 0.5$)		error/ (%)
	Present	Ansys		Present	Ansys		Present	Ansys		Present	Ansys	
1	24.4386	24.52	0.31	24.4184	24.50	0.31	24.3620	24.44	0.31	24.1957	24.271	0.31
2	61.7341	61.97	0.39	61.7093	61.95	0.39	61.6242	61.87	0.39	61.3568	61.60	0.39
3	118.9588	119.25	0.24	118.6711	118.97	0.25	117.9499	118.24	0.25	115.9943	116.28	0.25
4	188.0406	188.61	0.30	188.0336	188.6	0.30	188.0029	188.57	0.30	187.9056	188.48	0.31
5	277.0375	277.25	0.08	276.4685	276.68	0.08	275.0815	275.29	0.08	271.3751	271.57	0.07

Fig 8 shows the results of the influence of damage degree on the natural vibration frequency of circular curved beams solved by the method in this paper. In order to clearly compare frequency changes under different damage degrees, a double Y-axis diagram is adopted, with frequency value on the left and frequency change rate on the right (the relative variation of the natural frequencies between the damaged and the undamaged configurations). It can be seen from the figure that the frequency of each damage degree increases with the increase of order, but there is no significant difference. With the increase of damage degree, the relative frequency difference increases and is negative, indicating that the natural frequencies progressively decrease as the depth of the crack increases.
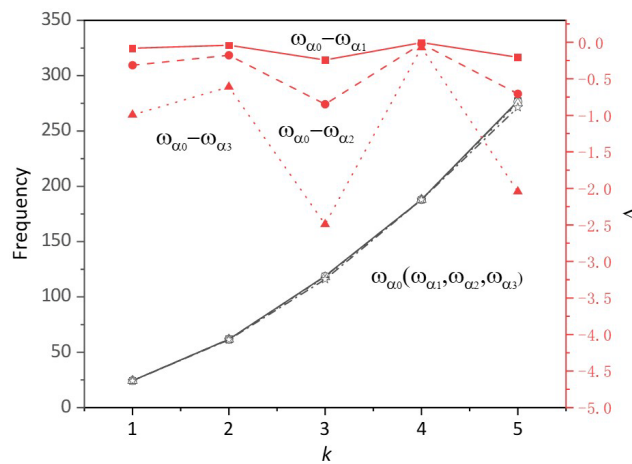
Figure 8 Influence of damage on natural vibration frequency of circular curved beam

In order to study the influence of crack location on the natural frequency of circular curved beam, the crack location changes uniformly every 10 degrees from left to right. As shown in Figure 9, the frequency value of damaged circular curved beam with $\alpha = 0.5$ is a function of single crack position β. It can be seen from the figure that due to the symmetry of the structure, the curve in the figure is a symmetric function curve. When the crack position is in the middle of the span, the first-order natural frequency of the circular curved beam reaches the maximum value, and when the crack position is 1/4 away from the side span, it reaches the minimum value.

Figures 10 show the relationship between the first four normalized frequency differences and the damage location β when the damage coefficient $\alpha = 0.5$. It can be seen from the figure that when the crack is located near the midspan, the first-order natural frequency difference is negative, which indicates that the first-order natural frequency of the circular curved beam increases after the midspan damage, which may be different from what we considered before.

Similarly, when the damage location is at 1/4 span, the second-order frequency difference is negative. However, the case that the frequency of the damaged structure is higher than that of the undamaged structure only exists in the first two frequencies, and ANSYS has a good corresponding relationship with the solution in this paper.
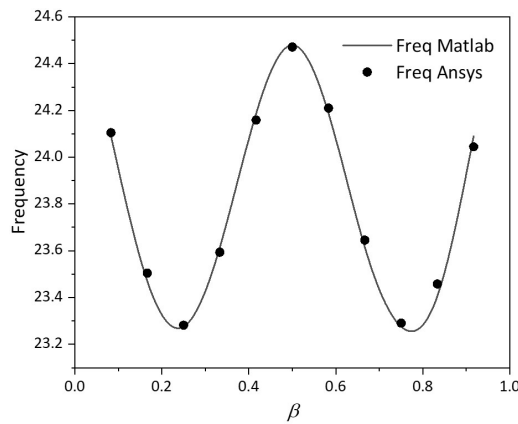
Figure 9 First natural frequency values at different crack locations $\left(\alpha = 0.5 \right)$
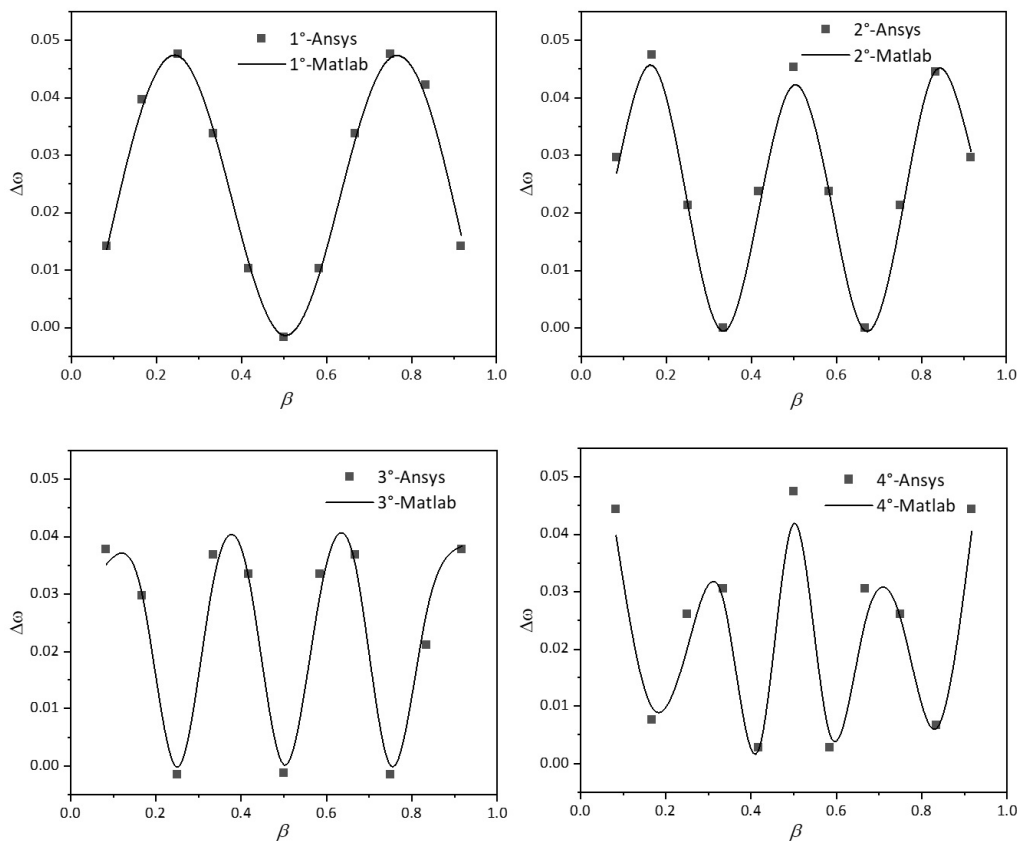
Figure 10 First four order normalized natural frequency difference $\Delta \omega \left(\alpha = 0.5 \right)$

In order to explore the abnormal phenomenon of damage on the first four natural frequencies of circular curved beams, the increase of damage coefficient a is considered at the abnormal positions of the first and third natural frequencies, as shown in Figure 11. It is worth noting that the damage degree does not change the phenomenon. In order to justify this unexpected behaviour, it can be seen from the comparison with other literatures that the solution in this paper considers not only the reduction of the stiffness of the damaged structure, but also the reduction of its mass, because the reduction of the damaged section will change the mass matrix, resulting in the change of the overall mass of the structure. As assumed in Krawczuk and Ostachowicz (1997), the occurrence of crack damage only leads to the

change of stiffness, while the overall quality of the structure remains unchanged. The same assumption is also made in Caliò et al. (2016). This provides a way to solve the unexpected behaviour of structure.

As shown in Figure 12, It is assumed that the crack only changes the stiffness of the element, whereas the mass of the element remaining unchanged. the mass reduction has been balanced by means of supplementary concentrated masses uniformly applied in the damage zones. It can be seen that in the first and third natural frequencies, the presence of the supplementary mass eliminates the region of frequency reduction, because all the curves have now positive values.
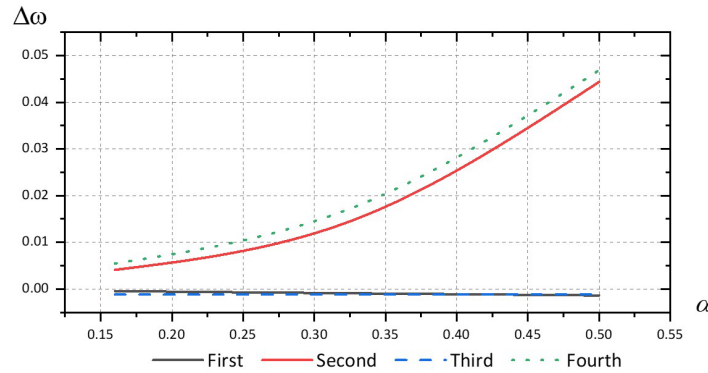
Figure 11 The first four normalized frequency difference of damage increase in the midspan of circular curved beam
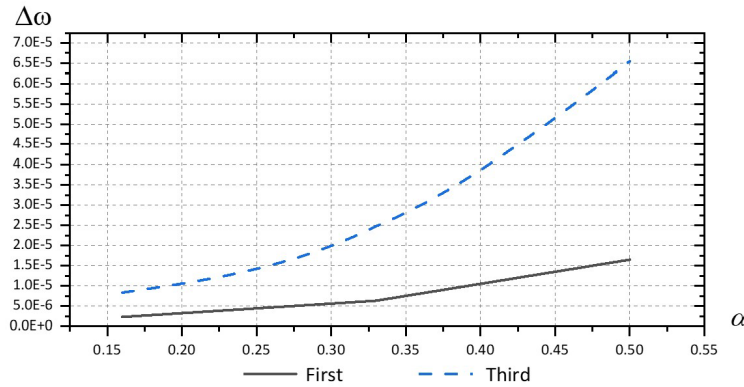
Figure 12 Variation of the first and third natural frequencies with the damage location with supplementary mass

3.2 Disturbance influence of damage on vibration modes

The first and fourth order modal solutions of α=0 and α=0.5 are obtained by using the method presented in this paper, as shown in Fig 13. By comparing the mode shape changes of circular curved beam in undamaged and several damaged configurations, it can be seen that the mode changes are greatly affected at the damage position, and the rotational displacement θ_z has the most obvious effect. Because the stiffness weakening caused by the crack is located at the 13th element, close to the right bearing, its effect on the rotational displacement of the right endpoint is more evident than that left endpoint. The results of the numerical calculations confirm the usefulness of the method used for the modal changes of circular curved beams with damage.

(a) First mode
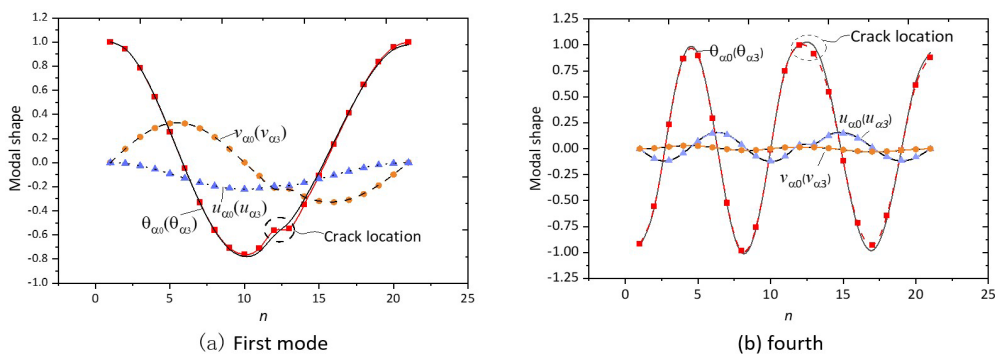
(b) fourth

Figure 13 Vibration modes of circular curved beam with demage in undamaged and α_3 -damaged

In order to show the influence of damage to modes more directly, Fig 14-16 shows the different curves of each mode of the first and fouth order. It is obvious that the damaged area has a significant influence on the modes change. The larger the damage coefficient, the more severe the damage disturbance to the vibration mode, and the damage has a certain impact on each vibration mode component, among which the numerical impact on the rotational displacement θ_z is the largest. By analyzing the difference curve of vibration modes of each order, it can be seen that the method in this paper has good applicability to analyzing the free vibration of circular curved beams with damage. In this paper, the method is programmed by Matlab mathematical calculation software, and the material parameters and geometric parameters of each region are expressed in sections. The purpose of solving the dynamic characteristics of circular curved beams with damage is achieved by controlling the parameters.
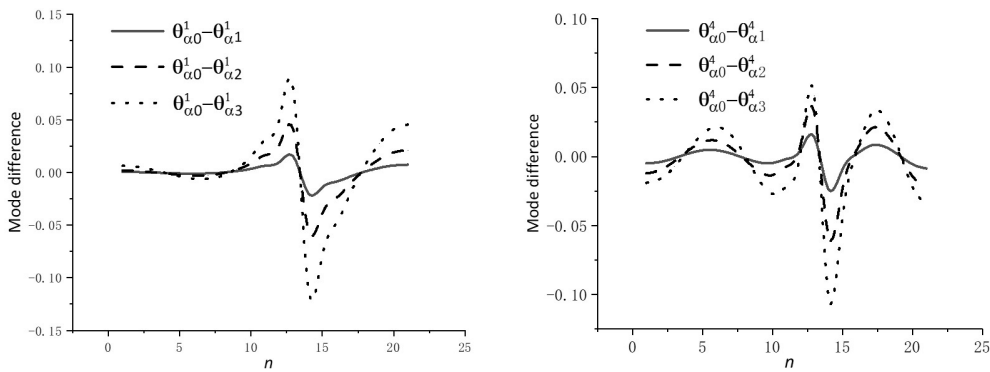
Figure 14 Rotational mode difference (k=1, k=4)
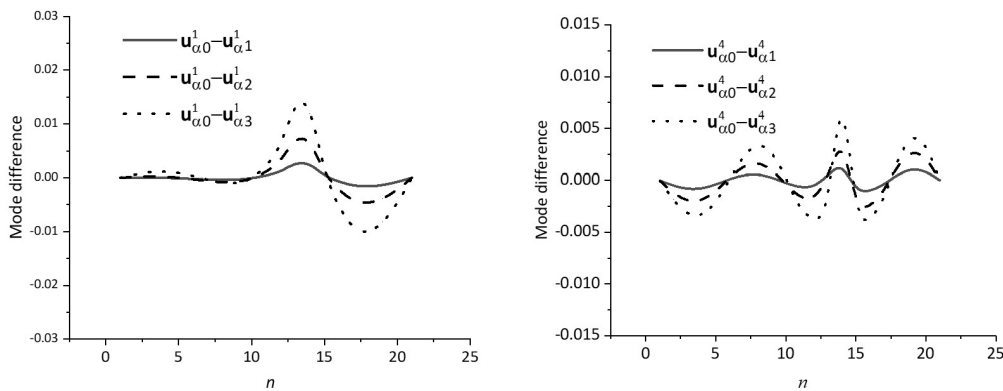
Figure 15 Radial mode difference (k=1, k=4)
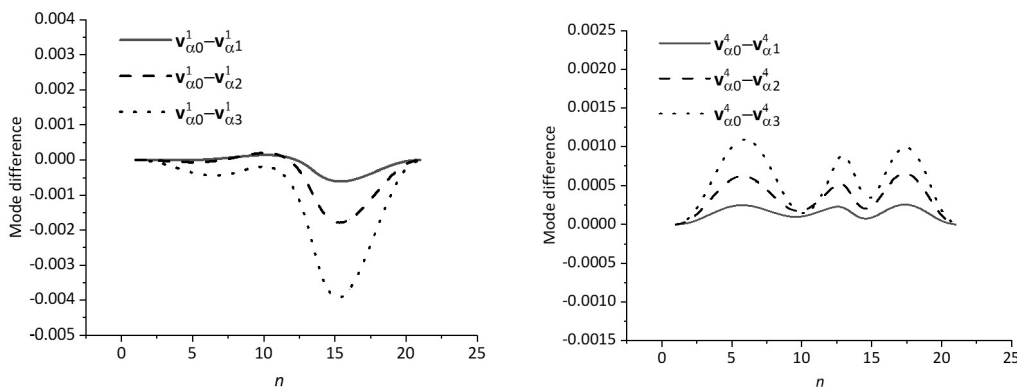
Figure 16 Tangential mode difference (k=1, k=4)

4 CONCLUSION

This paper establishes the mathematical model of circular curved beam with damage, simulates the damage state of circular curved beam by controlling the parameter changes, solves the free vibration problem of circular curved beam

with damage, obtains the self-oscillation frequency and vibration shape solution affected by the damage, compares the analysis results with the finite element calculation results for verification, and obtains the following conclusions:

(1) By comparing the finite element numerical calculation results, it can be seen that accurate solutions of self-oscillation frequencies and vibration patterns can be obtained by using this paper. Since the finite element method does not take into account the coupling effect between the non-adjacent nodes, which leads to the overall rigidity of the calculation results and affects the solution process requiring high precision error limits, this paper provides a semi-analytical method to improve the solution accuracy and has better adaptability for analyzing the dynamic characteristics of circular curved beams with crack damage.

(2) The results show that with the increase of the damage degree, the natural frequency of the circular curved beam decreases gradually, and the disturbance to the vibration mode becomes stronger, especially for the rotation displacement θ_z. The crack location has a significant effect on the natural frequency. In the existing damage model, when the crack is located in the middle of the span, the first and third natural frequencies show unexpected behavior, which is independent of the damage strength. The mass reduction has been balanced by means of supplementary concentrated masses uniformly applied in the damage zones and satisfactory results are obtained. Through the study of the positive problem of damage identification, the suitability of the semi-analytical solution for solving the natural frequency and mode of vibration of in-plane circular curved beams with damage is verified.

Author's Contributions: Conceptualization, XF Li and ZY Pan; Methodology, XF Li and ZY Pan; Investigation, XF Li, ZY Pan, HS Zhai and DY Zhao; Writing - original draft, XF Li, ZY Pan and HS Zhai; Writing - review & editing, XF Li, ZY Pan and DY Zhao; Resources, XF Li and ZY Pan; Supervision, XF Li.

Editor: Marco L. Bittencourt

References

Al-Said, S. M. (2008). Crack Detection in Stepped Beam Carrying Slowly Moving Mass. Journal of Vibration and Control, 14(12), 1903-1920. Retrieved from <Go to ISI>://WOS:000261242800005.

Anifantis, N., & Dimarogonas, A. (1983). Stability of columns with a single crack subjected to follower and vertical loads. International Journal of Solids and Structures, 19(4), 281-291. Retrieved from <Go to ISI>://WOS:A1983QH88300001.

Caliò, I., Greco, A., & D'Urso, D. (2016). Structural models for the evaluation of eigen-properties in damaged spatial arches: a critical appraisal. Archive of Applied Mechanics, 86(11), 1853-1867. Retrieved from <Go to ISI>://WOS:000386338700006.

Cerri, M. N., Dilena, M., & Ruta, G. C. (2008). Vibration and damage detection in undamaged and cracked circular arches: Experimental and analytical results. Journal of Sound and Vibration, 314(1-2), 83-94. Retrieved from <Go to ISI>://WOS:000256195100007.

Chondros, T. G., Dimarogonas, A. D., & Yao, J. (1998). A continuous cracked beam vibration theory. Journal of Sound and Vibration, 215(1), 17-34. Retrieved from <Go to ISI>://WOS:000075276300002. doi:DOI 10.1006/jsvi.1998.1640.

Chondros, T. G., Dimarogonas, A. D., & Yao, J. (2001). Vibration of a beam with a breathing crack. Journal of Sound and Vibration, 239(1), 57-67. Retrieved from <Go to ISI>://WOS:000166362500004.

Christides, S., & Barr, A. D. S. (1984). One-Dimensional Theory of Cracked Bernoulli-Euler Beams. International Journal of Mechanical Sciences, 26(11-12), 639-648. Retrieved from <Go to ISI>://WOS:A1984AEE2300010.

Dessi, D., & Camerlengo, G. (2015). Damage identification techniques via modal curvature analysis: Overview and comparison. Mechanical Systems and Signal Processing, 52-53, 181-205. Retrieved from <Go to ISI>://WOS:000345472500013.

Dimarogonas, A. D. (1996). Vibration of cracked structures: A state of the art review. Engineering Fracture Mechanics, 55(5), 831-857. Retrieved from <Go to ISI>://WOS:A1996VT65400010.

Douka, E., & Hadjileontiadis, L. (2005). Time-frequency analysis of the free vibration response of a beam with a breathing crack. Ndt & E International, 38(1), 3-10. Retrieved from <Go to ISI>://WOS:000225514700002.

Eroglu, U., & Tufekci, E. (2017). Crack modeling and identification in curved beams using differential evolution. International Journal of Mechanical Sciences, 131, 435-450. Retrieved from <Go to ISI>://WOS:000412960000040.

Friswell, M. I., & Penny, J. E. T. (2002). Crack Modeling for Structural Health Monitoring. Structural Health Monitoring-an International Journal, 1(2), 139-148. Retrieved from <Go to ISI>://WOS:000209200800002.

Hu, J. S., Feng, X., &Zhou, J. (2007). State-of-art of vibration analysis and crack identification of cracked beams. Journal of Vibration and Shock (11), 146-152+189. doi:10.13465/j.cnki.jvs.2007.11.028.

Karaagac, C., Ozturk, H., & Sabuncu, M. (2011). Crack effects on the in-plane static and dynamic stabilities of a curved beam with an edge crack. Journal of Sound and Vibration, 330(8), 1718-1736. Retrieved from <Go to ISI>://WOS:000287911000012.

Khdeir, A. A., & Reddy, J. N. (1997). Free and forced vibration of cross-ply laminated composite shallow arches. International Journal of Solids and Structures, 34(10), 1217-1234. Retrieved from <Go to ISI>://WOS:A1997WL75800004.

Krawczuk, M., & Ostachowicz, W. (1997). Natural vibrations of a clamped-clamped arch with an open transverse crack. Journal of Vibration and Acoustics-Transactions of the Asme, 119(2), 145-151. Retrieved from <Go to ISI>://WOS:A1997WW04400001.

Krishnan, A., Dharmaraj, S., & Suresh, Y. J. (1995). Free-Vibration Studies of Arches. Journal of Sound and Vibration, 186(5), 856-863. Retrieved from <Go to ISI>://WOS:A1995TB93200010.

Rice, J. R., & Levy, N. (1972). The part-through surface crack in an elastic plate. Journal of Applied Mechanics, 39, 185-194.

Rezaiee-Pajand, M., & Gharaei-Moghaddam, N. (2020). Force-based curved beam elements with open radial edge cracks. Mechanics of Advanced Materials & Structures, 27(2), 128–140.

Pau, A., Greco, A., & Vestroni, F. (2011). Numerical and experimental detection of concentrated damage in a parabolic arch by measured frequency variations. Journal of Vibration and Control, 17(4), 605-614. Retrieved from <Go to ISI>://WOS:000289075800011.

Petroski, H. J. (1981). Simple Static and Dynamic-Models for the Cracked Elastic Beam. International Journal of Fracture, 17(4), R71-R76. Retrieved from <Go to ISI>://WOS:A1981MH13900014.

Qatu, M. S. (1993). Theories and Analyses of Thin and Moderately Thick Laminated Composite Curved Beams. International Journal of Solids and Structures, 30(20), 2743-2756. Retrieved from <Go to ISI>://WOS:A1993LV39700002.

Raveendranath, P., Singh, G., & Pradhan, B. (2000). Free vibration of arches using a curved beam element based on a coupled polynomial displacement field. Computers & Structures, 78(4), 583-590. Retrieved from <Go to ISI>://WOS:000089710900007.

Shen, M. H. H., & Pierre, C. (1990). Natural-Modes of Bernoulli-Euler Beams with Symmetric Cracks. Journal of Sound and Vibration, 138(1), 115-134. Retrieved from <Go to ISI>://WOS:A1990CZ71600008.

Sun, Z., Wang, D., & Li, X. (2021). Isogeometric free vibration analysis of curved euler-bernoulli beams with particular emphasis on accuracy study. International Journal of Structural Stability and Dynamics, 21(1), 2150011.

Tong, X., Mrad, N., & Tabarrok, B. (1998). In-plane vibration of circular arches with variable cross-sections. Journal of Sound and Vibration, 212(1), 121-140. Retrieved from <Go to ISI>://WOS:000073576800008.

Tseng, Y. P., Huang, C. S., & Kao, M. S. (2000). In-plane vibration of laminated curved beams with variable curvature by dynamic stiffness analysis. Composite Structures, 50(2), 103-114. Retrieved from <Go to ISI>://WOS:000088146400001.

Viola, E., Artioli, E., & Dilena, M. (2005). Analytical and differential quadrature results for vibration analysis of damaged circular arches. Journal of Sound and Vibration, 288(4-5), 887-906. Retrieved from <Go to ISI>://WOS:000232878000006.

Wang, Y. L., Ju, Y., Zhuang, Z., & Li, C. F. (2018). Adaptive finite element analysis for damage detection of non-uniform Euler-Bernoulli beams with multiple cracks based on natural frequencies. Engineering Computations, 35(3), 1203-1229. Retrieved from <Go to ISI>://WOS:000434649400005.

Zhu, Z. H., & Meguid, S. A. (2008). Vibration analysis of a new curved beam element. Journal of Sound and Vibration, 309(1-2), 86-95. Retrieved from <Go to ISI>://WOS:000251622100007.

Zhao, Y. Y., Kang, H. J., Feng, R., & Lao, W. Q. (2006). Research progress of curved beam. Advances in Mechanics, 2(2),170-186.